

# ILLUMINATION PROPERTIES AND GADGET EFFICIENCY STEADINESS OF WLEDS BASED ON QUANTUM DOTS

*Hsiao-Yi Lee<sup>1</sup>, Thinh Cong Tran<sup>2</sup>, Sang Dang Ho<sup>2,\*</sup>*

<sup>1</sup>Department of Electrical Engineering, National Kaohsiung University of Sciences and Technology, Kaohsiung, Taiwan.

<sup>2</sup>Faculty of Electrical and Electronics Engineering, Ton Duc Thang University, Ho Chi Minh City, Vietnam

\*Corresponding Author: Sang Dang Ho (email: hodangsang@tdtu.edu.vn)  
 (Received: 14-April-2024; accepted: 09-October-2024; published: 31-December-2024)  
<http://dx.doi.org/10.55579/jaec.202484.459>

**Abstract.** *The recent improvements in picture quality have led to the need for new methods to create displays that meet more rigorous standards. While the screen market is mainly dominated by liquid crystal display (LCD) and light emitting diode (LED) technology, these technologies have downsides solvable via creating augmented electroluminescent screens. Utilizing sticky quantum dots (QDs) in the form of down transmuters facilitates creating screens featuring highly improved chroma clarity as well as range. As such, sticky nanocrystals prove a promising option when it comes to creating electroluminescent devices, providing a simple way to build high-quality displays. The QDs that emit light featuring significant fluorescent quantum output along with chroma clarity covering the entire visible spectrum, as well as significantly-bright singular-chroma LED apparatuses featuring extrinsic quantum proficiencies reaching 1.30%, 0.39%, 1.04%, and 2.10% respectively in the case of blue, red, orange, and green hues, saw the prospect of development. Additionally, white LEDs were created by combining QDs, achieving a color temperature of 5,300 K and over 80% color rendering index. The LED performance is also extensively evaluated, including color stability, and device efficiency, providing crucial data*

*for the advancement of high-quality electroluminescent displays.*

**Keywords:** *White LED, Lambert-Beer law, color rendering index, luminous efficacy.*

## 1. Introduction

In recent years, the demand for high-performance displays has intensified, driven by advancements in picture quality, color rendering, and energy efficiency. Traditional display technologies, such as liquid crystal displays (LCDs) and light-emitting diodes (LEDs), while widely adopted, face several limitations, particularly in terms of color purity, contrast, and device efficiency. These limitations have spurred the development of next-generation electroluminescent screens, where colloidal quantum dots (QDs) have emerged as a transformative technology. Colloidal quantum dots (QDs) have piqued the scientific community's interest because of their discovery [1] due to their distinctive characteristics, making them appropriate for many different uses, such as healthcare [2, 3] or optoelectronics [4, 5]. Colloidal QDs have lately been used to build very effective photovoltaic gad-

gets [6–9], photodetectors [10–13], and diodes emit illumination (LEDs) [10] due to their superior semiconductor characteristics. Due to their very elevated fluorescence, quantum produces ( $\Phi_f \approx 1$ ), hue adjustability according to particle size and structure, highly restricted emitting spectra, and elevated heating and photostability [11], observable-illumination-generating QDs having core-shell configuration are ideal options for the creation of gadgets emit illumination.

QDs, with their distinctive optical properties, including high fluorescence quantum yields, size-tunable emission spectra, and exceptional color purity, offer a promising solution to the challenges faced by current display technologies. QDs are currently used when it comes to creating screens featuring significant chroma clarity as well as extensive chroma scale, but these screens rely on LCD and LED technologies. In this setup, diodes emit blue light for backlighting, while QD units, usually emitting red as well as green light, serve in the form of down transmuters for generating various chromas. While LCD LED technologies provide extremely bright illumination, the use of QDs allows for display units featuring significant chroma clarity as well as extensive chroma scale. Regardless, the backlighting used for said approach hinders the clarity for black, influencing picture contrast, and also increases the overall thickness of the panel. To overcome these limitations, augmented proficient display units should be capable of comprising a matrix featuring independently controllable multi-color pixels, similar to organic LED(OLED)technology, but utilizing inorganic colloidal QDs to emit light [13]. Currently, QDs are used to produce electroluminescent apparatuses featuring outstanding extrinsic quantum proficiency as well as significantly expanded chroma range due to the excellent chroma clarity for the discharged illumination. Additionally, because black color is produced by inactive pixels, the picture contrariety for in OLED as well as QDLED electroluminescent apparatuses would significantly surpasses current methods using backlighting.

Substantial progress has been made over the past decade not just in producing elevated-standard QDs with emission spanning the whole observable spectrum, but additionally in con-

structing extremely effective gadgets emitting illumination. Mashford et al. stated in 2013 that by utilizing an inverted gadget architecture and core-shell CdSe/CdS QDs for the emitted layer, they were able to fabricate LEDs producing red hue with the present effectiveness of  $19 \text{ CdA}^{-1}$  and an excellent EQE of 18% [14]. A similar time, Lee et al. stated the gadgets' production that emit blue utilizing CdZnS/ZnS QD units within one typical arrangement employing PEDOT:PSS in the form of one cavity-administrating sheet (CAS), PVK like a hole transport substances (HTS), and ZnO nanoparticles to be an electron transfer substance (ETM), which illustrated a highest illumination reaching  $2,624 \text{ Cdm}^{-2}$ , a present effectiveness reaching  $2.2 \text{ CdA}^{-1}$ , as well as extrinsic quantum proficiency reaching 7.1% [15]. A work of Lee's team focused on the synthesis of multi-shell emits green hue CdSe/ZnS/ZnS QD units as well as the following construction for gadgets featuring a present effectiveness reaching  $46.4 \text{ CdA}^{-1}$  as well as extrinsic quantum proficiency reaching 12.6% [16]. A work of Yang's team reported the reported the fabrication gadgets that emit red, green, blue illumination in 2015, with the highest operations/extrinsic quantum proficiency reaching  $15 \text{ CdA}^{-1}/12.0\%$  in the case red gadgets,  $63 \text{ CdA}^{-1}/14.5\%$  in the case of green one, as well as  $4.4 \text{ CdA}^{-1}/10.7\%$  in the case of blue ones [16]. Lee et al. published a paper in 2015 detailing the manufacture of gadgets emitting white illumination (WLEDs) according to red, green, as well as blue (RGB) blended QD sheets displaying remarkable effectiveness: a brightness reaching  $23,352 \text{ Cdm}^{-2}$ , a present effectiveness reaching  $21.8 \text{ CdA}^{-1}$  as well as extrinsic quantum proficiency reaching 10.9% [17].

Previous studies have focused on creating high-efficiency LEDs using QDs and overcoming their limitations. However, for practical applications and commercialization, a deeper understanding of key factors is needed. These factors include stability under working conditions, the causes and processes of electroluminescence (EL) decay, the duration of on-off operation, and the development of illumination properties over extended periods [18]. Furthermore, several methods for producing white LEDs with

programmable illumination characteristics have been proposed. These methods include:

1. Mixing multiple QDs to control their emission ratios;
2. Developing improved sedimentation techniques for patterned films containing various QDs;
3. Embedding QDs in an insulating polymer matrix to prevent photoluminescence (PL) decay, although this reduces sheet conductivity;
4. Using QD compounds as phosphors, which requires the presence of shorter-wavelength backside-lighting LEDs.

Shortly, quantum dot-based LEDs (QD-LEDs) are potential to significantly outperform existing backlighting systems used in LCDs, which suffer from suboptimal contrast and color accuracy. The unique properties of QDs allow for the fabrication of electroluminescent devices with unparalleled color purity and broad spectral coverage, making them an ideal candidate for the next generation of ultra-thin, high-brightness displays. Hence, in this work, to maximize the prospect of QD-LEDs, we modified traditional processes to create extremely bright core-shell QDs that emit illumination having varied chemical components. Furthermore, we created and thoroughly tested not just the matching sole-hue LEDs, but additionally the WLEDs created by combining RGB or orange, green, and blue (OGB) QDs. This research also addresses the critical need for deeper understanding and optimization of QD-WLEDs, particularly in terms of color stability, and device efficiency, contributing to driving innovation in the field of optoelectronics.

## 2. Experimental

**Materials:** The whole substances used in this project were obtained from commercial providers. The following forerunners and solvents were obtained from Sigma-Aldrich: CdO (99.99%), Zn(OAc)<sub>2</sub> (99.99%), oleic acid (OA)

(90 %), S (99.99%), Se (99.99%), 1-octadecene (ODE) (90%), trioctylphosphine (TOP) (90%), hexane ( $\geq 95\%$ ), acetone ( $\geq 99.9\%$ ), and ethanol (absolute). Thin Film Devices supplied prepatterned indium tin oxide (ITO) substrates. Heraeus Clevios supplied the PEDOT:PSS (Al4083), while Sigma-Aldrich supplied the PVK and Al:ZnO nanoparticles.

**QDs' preparation:** A two-step hot injection approach was utilized to create blue-illumination CdZnS/ZnS QDs [19]. CdSe/CdS/ZnS QDs producing green, orange, and red illumination were produced using one sole-stage hot injection process with minor changes.

**Gadget design:** The ITO substrates were sonicated for 5 minutes in a soap solution. The substrates were subsequently washed twice, once with Milli-Q water and once with ethanol. After that, place them in a solvent containing isopropanol:acetone (1:1 v/v) and sonicated within 5 minutes. Next, clean them with ethanol, and pressure and dry them in air. The substrates were placed in a UV-O<sub>3</sub> cleaning for 30 minutes, and a PEDOT:PSS solution was spun-cast at 3,000 rpm during 60 seconds before being treated at 150<sup>0</sup>C during 30 minutes in air to produce a thin film (20 nm). Following that, a PVK film was applied by spin-casting a solution of 10 mg·mL<sup>-1</sup> PVK in chlorobenzene for 60 seconds and heated in air at 150<sup>0</sup>C within 30 minutes. The QD solutions (5 mg·mL<sup>-1</sup>) in hexane were then molded into fibers for 20 seconds. The widely supplied Al:ZnO nanoparticle solution was then molded into fibers on the QD sheets at 1,500 rpm for 20 seconds before being heated in air at 100<sup>0</sup>C lasting 5 minutes. Lastly, aluminum top electrode was thermal vaporized with rate of  $1.5 - 2 \text{ \AA} \cdot \text{s}^{-1}$ ; the activating portions were encased with Lighting Enterprises UV photocurable epoxy resin and a cover glass.

By rotational molding the appropriate substances, we utilized the typical gadget design. To build the gadgets, a PEDOT:PSS film was coated as the HIL over a pre-patterned ITO substrate. The HTM was then formed by depositing a thin film of PVK, and then consecutive rotational molding of the QDs in hexane (5·mL<sup>-1</sup>). To be ETM and hole-blocking sheet, Al:ZnO nanoparticles were utilized. Lastly, above the

Al:ZnO film, an aluminum electrode was heat vaporized. In order to prevent early deterioration, the operational portion of the gadgets was enclosed in an epoxy resin in a glovebox.

### 3. Results and discussion

It is an elevated-resolution transmittance electron microscopy (HR-TEM) picture showing blue quantum dots (QDs) with a fairly uniform size distribution, all less than 10 nm in diameter. The uniformity for blue QD units' size within the HR-TEM visuals would be supported through photoluminescence (PL) spectra, possessing a whole breadth under half maxima reaching just 24 nm. The findings of power-scattered X-ray research verify QDs' various element components. Moreover, judging by said visuals, blue QD units appear to have a greater globular property, surpassing other QDs, likely due to the different synthesis methods used. After creating and describing the visible-light-emitting QDs, various types of multi-color LEDs were manufactured and thoroughly examined utilizing QD units in the form of illumination-generating materials.

When describing the chroma characteristics in white illumination means, the illumination industry uses two key measurements: correlated chromatic heat (CCT) as well as chroma rendition indicator (CRI) [20]. The chromatic temperature (CT) in illumination means would be the Kelvin heat where fired black body radiators' color connects to the chroma in illumination means. Black bodies turn red under small temperatures at first, becoming blue-white under extremely significant temperatures. Incandescent bulbs can be estimated using the chroma temperature in black bodies since their tungsten filaments emit light at high temperatures. Nevertheless, fluorescent supplies or WLEDs use alternative physical concepts for producing white illumination, necessitating a more specific description of the hue heat. CCT would be the heat from said radiators with the same hue as the illumination generated by the supply.

Warm white illuminations with CCTs below 3,200 K are intended to exhibit yellow-orange

tones. Lights with a CT between 3,200 and 4,000 K are regarded as balanced, whereas cool white lights have blue-white tones with CCTs above 4,000 K. CCT does not reveal the lighting's spectral dispersion, while being a strong indicator of how light would seem overall. It is important to note that changing the QD proportions might modify the CCT of QD-WLEDs. The CRI was created to give a more precise measurement of a white light source's spectral energy distribution. When compared to a standard light of the same CT, CRI evaluates how well a white light source reproduces colors. An item lit with two white lights with the same CCT but differing CRIs may seem very different because of the distinct spectral power distributions. Light sources with CRI scores higher than 80% are typically thought to have superior color rendition capabilities.

The consistency of the white light produced by WLEDs is an important factor to consider. In our research, we studied the development of color characteristics (CCT- CRI) using different methods. We looked at the QD-WLEDs' EL spectra made with RGB and OGB methods. Both approaches produce devices that generate light that spans the visible spectrum, despite the various forms of the spectra. Green and orange QD emissions are produced by the OGB devices, which have a wide signal between 500 and 700 nm and a peak at 471 nm, whereas the RGB devices have three distinct peaks at 471, 552, and 642 nm.

Developing green QDs with superior color characteristics is a potential easy method to raise the CRI of QD-WLEDs. This would increase the range of white light that is generated and raise the CRI. Excessive color gamut expansion, however, can result in oversaturated hues and alter how the human eye perceives color. In order to achieve higher quality nanocrystals with greater radiative recombination at the expense of nonradiative routes, the primary technique for increasing EQE is to modify the experimental conditions for QD synthesis.

For the further investigations into the color stability and illumination efficiency of the QD-LED devices in the work, the connection of particle size and scattering and conversion perfor-

mance are discussed. Fig. 1 demonstrates the connection between particle sizes and light distribution. Increasing particle sizes can enhance wavelength conversion efficiency and light transmission, leading to increased brightness as forward scattering and reabsorption of blue light decrease and forward emission blue light dispersion increases. This can be achieved by decreasing the amount of yellow phosphorus while increasing the particle sizes. Additionally, the corresponding color temperature (CCT) is less likely to change. Fig. 3 and Fig. 4 demonstrate that CCT is not concentration-dependent, as there is an increase in YGA:Ce yellow phosphor as particle sizes increase. In contrast to Fig. 2, which shows a decrease in the YGA:Ce dosage, these figures show a decrease in the yellow phosphor particle sizes.

When the YGA:Ce phosphor ratios are lower (over 27% to just over 25%), the particle sizes depicted in Figure 2 are higher (between 1 and 10  $\mu\text{m}$ ). Furthermore, Fig. 3 shows how more doping can reduce the phosphor's CCT variance. CCT values are maximum when particle sizes are 4-6  $\mu\text{m}$  at temperatures about 3050 K. Figure 4 shows that the D-CCT finally reaches its lowest value at 9  $\mu\text{m}$  of particle sizes, which is approximately 230 K lower than the results at 5  $\mu\text{m}$  of particle sizes, where the D-CCT value is approximately 270 K. Fig. 5 indicates

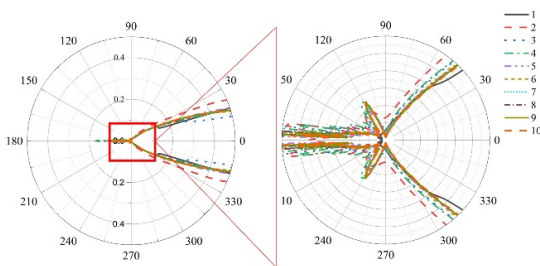


Fig. 1: Scattering coefficients with various particle sizes of 1  $\mu\text{m}$ -10  $\mu\text{m}$ .

that the particle sizes did not always increase the brightness of the white illumination generation. The best results were obtained when particle sizes of 9  $\mu\text{m}$  were used, while the least optimal outcomes were produced when particle sizes of 1  $\mu\text{m}$  were used. Increased backscattering and reabsorption are to blame for the reduced blue emission and unbalanced color distribution.

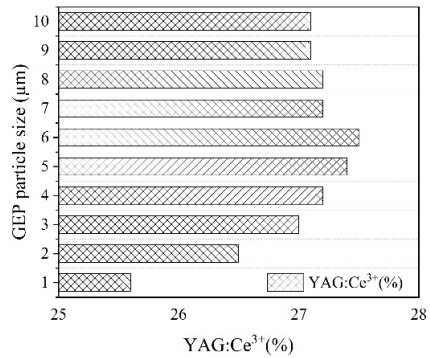


Fig. 2: YGA:Ce phosphor proportion coefficients at different particle sizes.

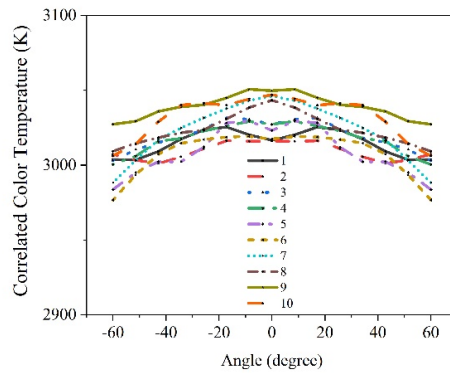


Fig. 3: CCT values with various particle sizes.

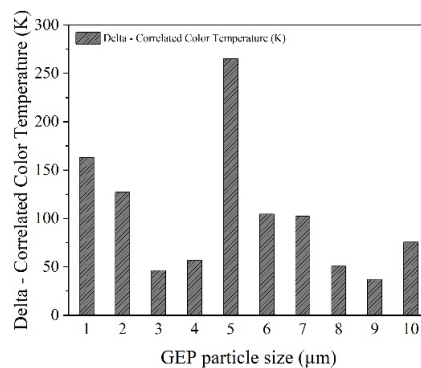
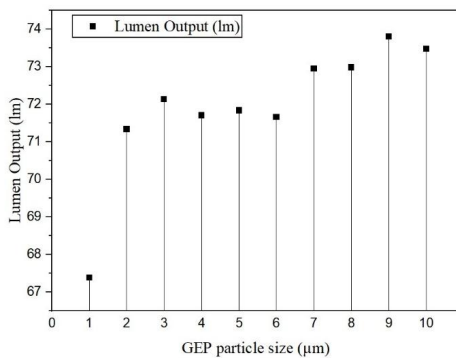


Fig. 4: Color difference values with various particle sizes.

When subjected to more blue light that has been backscattered, greater particle sizes would cause

the phosphor to shift from blue to yellow or orange-red. The phosphor coating cannot expand until the particle sizes reach a particular level. The emission spectrum would be limited due to the multiple reflections that the modified light would receive from various objects. In other words, a high phosphor dose may enhance CCT without diminishing luminous intensity by increasing the proportion of converted light that is back-reflected. As shown in Fig. 5, particle sizes of 9  $\mu m$  were found to be adequate for improving brightness and color uniformity in a simulated WLED with an output power of nearly 74  $nm$ .

The particle sizes shown in Fig. 6 and Fig. 7 have a significant impact on the brightness and color quality of white LEDs. Studies on color quality using the hue rendering indicator (CRI) and hue quality scale (CQS) demonstrated a constant decline as particle sizes increased to 10  $\mu m$ . This decrease in CRI and CQS could be attributed to the unpredictability of blue, green, and yellow-orange hues. Larger particle sizes result in better dispersion but lead to irregular light output, favoring the yellow-orange spectrum. We will change the CRI and CQS of this phosphor as we evaluate the data and consider additional factors such as particle size [21, 22]. Fig. 8 depicts the bands of lumi-



**Fig. 5:** Luminescence strength with various particle sizes.

nous strength. As shown, the particle sizes may enhance the blue and orange-red wavelengths of the white light spectrum. One can change the patterns of light scattering and absorption in particle sizes to improve lighting efficacy. The

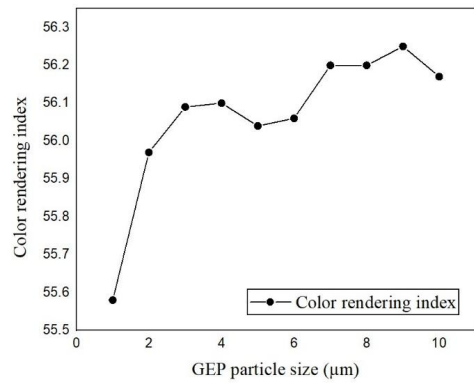


**Fig. 6:** CRI coefficients of the WLED at different particle sizes.

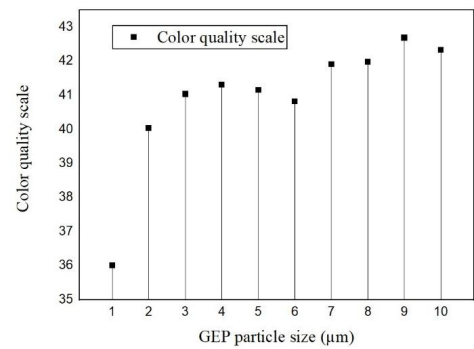


**Fig. 7:** CQS coefficients of the WLED at different particle sizes.

biggest peaks are found in the blue (about 450  $nm$ ) and yellow-orange (approximately 550  $nm$ ) wavelength ranges.

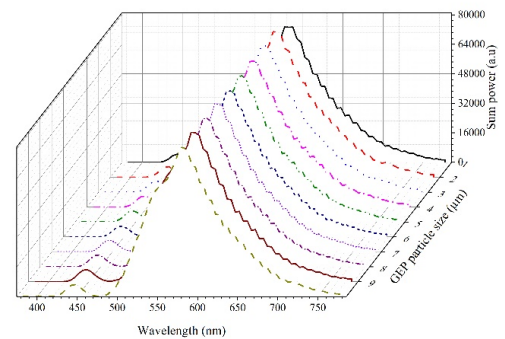


**Fig. 8:** Luminescence power of the WLED.

## 4. Conclusions

In our research, the efficient light-emitting devices that cover the entire visible spectrum were developed and assessed. These devices included white LEDs created using two different methods, RGB and OGB. From the attained data, it is possible to gain valuable insights into the performance of QD-WLEDs and identified processes responsible for changes in their white light properties. Firstly, the transfer of power and/or charges from quantum dots (QDs) with a larger bandgap to those with a smaller bandgap partially accounts for the reduced efficiency of RGB and OGB devices compared to single-color QD-LEDs. Additionally, we observed varying emission intensities of blue, green, orange, and red QD-LEDs leading to changes in the hue coefficients of RGB and OGB devices. It also found that QDs remain stable during extended operation ( $> 20$  hours) at a constant voltage, but the PEDOT:PSS/ITO interface deteriorates, leading to restricted charge injection into wider-bandgap QDs, thus shifting the white light properties towards the red end of the spectrum. These effects have not received much attention, and this study suggests that replacing PEDOT:PSS with a different HIL could lead to more stable devices and consistent white light properties. The studies on the connection between the particle size and illumination efficiency and chromaticity reveal that  $9 \mu\text{m}$  should be selected for the optimal performance of the device. These findings are crucial for the advancement of future ultrathin, high-brightness electroluminescent displays utilizing the wide color gamut offered by inorganic QDs.

## References

- [1] V.T. Pham, N.H. Phan, G.F. Luo, H.Y. Lee, and D.Q.A. Nguyen. The application of calcium carbonate  $\text{CaCO}_3$  and titania  $\text{TiO}_2$  for color homogeneity and luminous flux enhancement in PC-LEDs. *Adv. Eng. Comput.*, 5(2):75–82, 2021.
- [2] N.H.S. Dang, D.M.T. Nguyen, T.P.L. Nguyen, D.Q.A. Nguyen, , and H.Y. Lee. Enhance wleds performance with additional phosphor materials in multi-layer remote structure. *Adv. Eng. Comput.*, 5(3):167–176, 2021.
- [3] K. Desnijder, W. Deketelaere, W. Ryckaert, P. Hanselaer, , and Y. Meuret. Efficient design method of segmented lenses for lighting applications with prescribed intensity and low peak luminance. *Leukos*, 15(4):281–292, 2019.
- [4] W.H.Y. H. Cheng, Y. Feng, X. Chen, and Y. Wang. Luminance mapping of light sources using ray sampling and compression. *J. Mod. Opt.*, 67(2):99–110, 2019.
- [5] H.J. Choi. Design and fabrication of sub-micron period grating as an imprinted light guide plate for a backlight unit. *J. Inf. Disp.*, 20(4):239–247, 2019.
- [6] M.J. Sheu, Y.L. Liu, J.J. Wang, , and J.W. Pan. Design of a bi-directional illumination system for a dual view capsule endoscope. *J. Mod. Opt.*, 66(3):252–262, 2018.
- [7] M. Tanaka, T. Yamada, M. Shigeta, H. Komen, M. Fukahori, and N. Saito. Experimental study on effects of gas-shielding in lap-fillet arc welding. *Weld. Int.*, 35(10-12):492–507, 2021.
- [8] F. Li, Y. Zhao, H. Gao, D. Wang, Z. Miao, H.Cao, Z. Yang, and W. He. Doping white carbon black particles to adjust the electro-optical properties of PDLC. *Liq. Cryst.*, 48(15):2130–2139, 2021.
- [9] S.V. Mednikov, A.V. Valo, A.S. Ponomarev, and A.I. Burkhanov. Photochromic effect in piezoelectric ceramics PZT-19. *Ferroelectrics*, 561(1):36–43, 2020.
- [10] S. Lin, J. Yu, J. Cai, E. Chen, S. Xu, and Y. Ye. Design of a freeform lens array based on an adjustable Cartesian candela distribution. *J. Mod. Opt.*, 66(20):2015–2024, 2019.
- [11] T. Sezer, M. Altımsık, E.M. Guler, A. Kocyigit, H. Ozdemir, and A. Koytak. Evaluation of xenon, light-emitting diode (LED)

- and halogen light toxicity on cultured retinal pigment epithelial cells. *Cutan. Ocular Toxicol.*, 38(2):125–130, 2018.
- [12] O. Rabaza, D. Gomez-Lorente, A.M. Pozo, and F. Perez-Ocon. Application of a differential evolution algorithm in the design of public lighting installations maximizing energy efficiency. *Leukos*, 16(3):217–227, 2019.
- [13] C.N. Liao, H. Chiu, , and Y. Hsieh. Wide-range dimmable LED lighting based on QL-SEPIC converter. *Epe J.*, 29(1):25–37, 2018.
- [14] A. Pena-Garcia and A. Sedziwy. Optimizing lighting of rural roads and protected areas with white light: A compromise among light pollution, energy savings, and visibility. *Leukos*, 16(2):147–156, 2019.
- [15] J.D. Bullough, A. Bierman, and M.S. Rea. Evaluating the blue-light hazard from solid state lighting. *Int. J. Occup. Saf. Ergon.*, 25(2):311–320, 2017.
- [16] B. Aydn, A. Ozgur, H.B. Ozdemir, P.U. Gocun, M.A. Inan, and H.T. Atalay. Comparison of the effects of operating microscopes with light emitting diode and halogen light source on the eye: a rabbit study. *Cutan. Ocular Toxicol.*, 40(4):319–325, 2021.
- [17] M.A.B. Oliveira, M. Scop, A.C.O. Abreu, P.R.S. Sanches, and A.C. Rossim. Entrainment effects of variations in light spectral composition on the rest-activity rhythm of a nocturnal rodent. *Chronobiol. Int.*, 36(7):934–944, 2019.
- [18] A.V. Kuzmenko, A. S. Tverjanovich, M. A. Ilyushin, and Yu. S. Tveryanovich. The effect of the concentration of high-absorbing inclusions on the laser initiation threshold of energetic materials: model and experiment. *J. Energ. Mater.*, 37(4):420–432, 2019.
- [19] S. Hongkong and J. Jamradloedluk. A technique for evaluation of sky luminance distribution in tropical climate: a case study of Northeastern Thailand. *Int. J. Sustain. Energy*, 39(2), 2019.
- [20] N.S Okkels, L.G. Jensen, L.C. Skovshoved, R.A.A.B. Blicher, and E.Vieta. Lighting as an aid for recovery in hospitalized psychiatric patients: a randomized controlled effectiveness trial. *Nord. J. Psychiatry*, 74(2):105–114, 2019.
- [21] R.F. Babayeva and A.S. Abdinov. Photoconductivity in polyethylene-semiconductor (p-gase) composite. *Mol. Cryst. Liq. Cryst.*, 717(1):40–46, 2021.
- [22] B. Ozer and B. Guven. Energy efficiency analyses in a Turkish fabric dyeing factory. *Energy Sources. Part a, Recover. Util. Environ. Eff.*, 43(7):852–874, 2020.



## About Authors

**Hsiao-Yi LEE** was born in Hsinchu city, Taiwan. He has been working at the Department of Electrical Engineering, National Kaohsiung University of Science and Technology, Kaohsiung, Taiwan. His research interest is optics science.

**Thin Cong TRAN** received the Ph.D. degree in Electrical Engineering from VSB-Technical University of Ostrava, Czech Republic, in 2020. Presently, he is working as a lecturer at the Faculty of Electrical and Electronics Engineering, Ton Duc Thang University, Ho Chi Minh City, Vietnam. His research interests involve the optimization of the power system and applications of soft computing in control of electric machine drives and optics science. He can be contacted

at email: trancongthinh@tdtu.edu.vn.

**Sang Dang HO** was born in Ho Chi Minh City, Vietnam in 1973. He received the M.Ss. degree in Electrical Engineering from Ho Chi Minh University of Technology, Ho Chi Minh City, Vietnam in 2008, and received the Ph.D. degree in Electrical Engineering from VSB-Technical University of Ostrava, Czech Republic, in 2020. Presently, he is working as a lecturer at the Faculty of Electrical and Electronics Engineering, Ton Duc Thang University, Ho Chi Minh City, Vietnam. His research interests involve the optimization of the power system and applications of soft computing in control of electric machine drives and optics science.